

Global sensitivity analysis of (a)symmetric energy harvesters

João Pedro Norenberg · Americo Cunha Jr. · Samuel da Silva ·
 Paulo Sérgio Varoto

Received: date / Accepted: date

Abstract Parametric variability is inevitable in actual energy harvesters and can define crucial aspects of the system performance, especially in susceptible systems to small perturbations. In this way, this work aims to identify the most critical parameters in the dynamics of (a)symmetric bistable energy harvesters with nonlinear piezoelectric coupling, considering the variability of their physical and excitation parameters. For this purpose, a global sensitivity analysis based on the Sobol' indices is performed by an orthogonal decomposition in terms of conditional variances to access the dependence of the recovered power concerning the harvester parameters. This technique quantifies the variance concerning each parameter individually and jointly regarding the total variation of the model. The results indicate that the frequency and amplitude of excitation, asymmetric bias angle, and piezoelectric coupling at the electrical domain are the most influential parameters that affect the mean power harvested. It has also been shown that the order of importance of the parameters can change from stable conditions. In possession of this, a better

João Pedro Norenberg
 São Paulo State University, Ilha Solteira, SP, Brazil
 ORCID: 0000-0003-3558-4053
 E-mail: jp.norenberg@unesp.br

Americo Cunha Jr.
 Rio de Janeiro State University, Rio de Janeiro, RJ, Brazil
 ORCID: 0000-0002-8342-0363
 E-mail: americo.cunha@uerj.br

Samuel da Silva
 São Paulo State University, Ilha Solteira, SP, Brazil
 ORCID: 0000-0001-6430-3746
 E-mail: samuel.silva13@unesp.br

Paulo Sérgio Varoto
 São Paulo University, São Carlos, SP, Brazil
 ORCID: 0000-0002-1240-1720
 E-mail: varoto@sc.usp.br

understanding of the system under analysis is obtained, identifying vital parameters that rule the change of dynamic behavior and constituting a powerful tool in the robust design and prediction of nonlinear harvesters.

Keywords energy harvesting · nonlinear dynamics · sensitivity analysis · Sobol' indices · polynomial chaos expansion

1 Introduction

Novel technological applications that use small-scale autonomous devices continue to emerge every year. In this context, one of the significant challenges is the development of a self-sufficient machine, i.e., an electromechanical system capable of generating electrical power to sustain its consumption. In this perspective, energy harvesting is a prominent research area that comprises dispersed energy in the environment (e.g., solar, wind, heat, vibration, etc.) to convert into electricity.

Among the energy sources present in the environment, kinetic energy from structural vibration has been major explored for energy harvesting due to a good compromise between energy availability and ease of use. The literature has several recent works with powerful applications involving this idea, such as the generation of bio-cellular energy [30], medical implants [28], sensor power [50, 32, 54], and even osmotic energy [51]. The conversion techniques used in vibration energy harvesting are electrostatic [37], electromagnetism [5], and piezoelectricity [19], the latter being the most used due to high-density energy.

Broadly, energy harvesting systems are widely addressed as deterministic, where all parameters are free of uncertainty. However, real systems are subject to

manufacturing processes and environmental variability, remarking uncertainties associated with their material properties, geometry, and external conditions. Thus, disregarding these uncertainties is a major limitation of the deterministic approach, leading to low fidelity or even wrong predictions. Nowadays, engineering deals with robust and accurate predictions, hence often required to consider uncertainties. The discipline that studies the uncertainty effect is known as uncertainty quantification (UQ) [45], which relies on probability theory to determine the output distribution given the system's input distribution. UQ has special importance on energy harvesting to handle the low-scale and accurate models. Recent reviews of UQ in the latter context are found in [36, 33, 21].

Despite being a preliminary study in a broad UQ framework [38], sensitivity analysis (SA) can provide crucial and nontrivial insight into the behavior of a nonlinear system. In other words, it may aid in finding the parameters that most affect the system response. In this way, it has been receiving increasing attention in many engineering systems, giving a comprehensive approach to how an input data variation can affect the underlying system response [1].

Sensitivity analysis techniques can be classified as local and global [6]. The first is based on the approximation of the partial derivative to assess how the variation in one parameter affects the system's response, keeping other parameters fixed according to their nominal values. Alternatively, the second provides a comprehensive approach, as it assesses the effect of parameters varying within the entry space considered multidimensional. A useful survey on the state-of-the-art sensitivity analysis techniques is available at [42].

Applications of sensitivity analysis on energy harvesting can be seen in the recent work by Aloui, Larbi, and Chouchane [3, 4], in which the authors performed a global sensitivity analysis (GSA) on a linear bimorph piezoelectric energy harvester under base excitation with a mounted load resistance in series. In the work of Ruiz and Meruane [41], the system's sensitivity concerning the behavior of the frequency response function of the linear piezoelectric energy harvester is analyzed. Both studies concluded that the effects of piezoelectric material's physical properties are fundamental for model variation and draw attention to the need to propagate the uncertainties in piezoelectric energy harvesters. However, to the author's knowledge, there is a gap in GSA evaluations and explorations in a nonlinear energy harvesting system to provide quantitative terms of which parameters most affect the response for their variability.

Linear models have limited bandwidth around their fundamental resonance frequency, and to overcome this limitation, broadband nonlinear vibratory energy harvesters are explored. The first works to implement bistable nonlinearity in energy harvesting systems were Cottone, Vocca, and Gammaiton in [8], and then Erturk, Hoffmann and Inman in [18], showing a substantial increase in the generation of piezoelectric energy concerning the linear system in a wide frequency band. This energy harvester has become a classical system, being explored for its potential and rich dynamics [20, 7, 34, 27, 16, 15, 53]. Optimization problem to enhance the performance of an energy harvesting device is also developed in [12]. Therefore, in the framework of nonlinear dynamical systems, GSA can be a workable tool to reveal each parameter's uncertainty influence, mainly because nonlinear systems present high sensitivity to input parameter variations and have a complex dynamic with regular and chaotic behaviors. Then, a question arises about how a nonlinear energy harvesting system behaves when considering uncertainties in its parameters.

From this scenario, this work deals with the global sensitivity analysis of bistable energy harvesting systems. To well-approach the physical model and study various conditions, sources of uncertainties and nonlinearities are addressed, such as nonlinear electromechanical coupling, asymmetric potential, and a bias angle. Thus, a statistical model is designed through a probability distribution function of the load parameters. The aim is to verify and classify which system parameter most affects the variability of power harvested. Accordingly, simplify the probabilistic model by dimensionality reduction and solve the crucial question, for instance, when and how uncertainty affects. Therefore, this report provides a preliminary UQ background, identifying the most sensitive and negligible parameter effects. In addition, it understands the phenomenon studied by the analysis of interactions between variables, an essential step for robustness and optimization applications on bistable energy harvesters, working as training to determine only the features that are statistically more linked to the output data.

The rest of this manuscript is organized as follows. Section 2 presents the energy harvesting system of interest. The global sensitivity analysis of this nonlinear system is formulated in Section 3, and the Polynomial Chaos Expansion approach used to compute the Sobol indices is presented in Section 4. Section 5, the numerical experiments conducted to analyze the sensitivity of a bistable energy harvester are presented and discussed. Section 5.5 summarizes the main results obtained here and the uncertainties propagation of the systems. Finally, in Section 6, presents the important conclusions.

2 Bistable energy harvesting system

An illustration of the energy harvesting system of interest in this work can be seen in Fig. 1, which consists of a rigid base excited by a harmonic force and a vertical fixed-free beam made of ferromagnetic material with two permanent magnets located near the bottom part of the base. In the beam upper part, high deformation region, a pair of piezoelectric layers is coupled to a resistive circuit responsible for converting the kinetic energy into electrical energy, dissipated in the resistor. The harvester has a bias, which leads to oscillates over a certain angle ϕ . Parameter ϑ can adjust the configuration of different potential energy functions, allowing to induce an asymmetric potential.

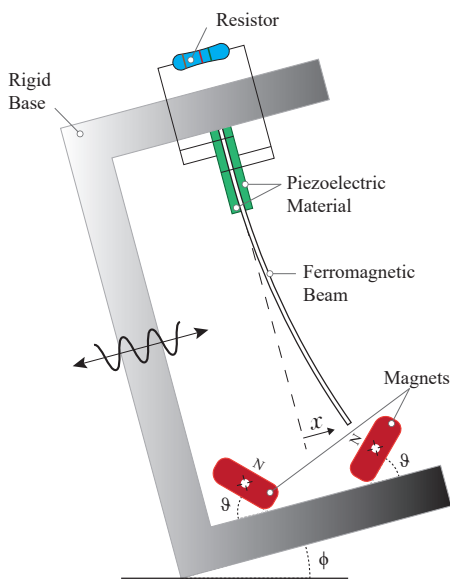


Fig. 1: Schematic illustration of the Piezo-Magneto-Elastic beam energy harvester.

If the bias angle is removed, the system becomes the classical piezo-magneto-elastic beam energy harvester proposed by Erturk, Hoffmann, and Inman [18]. Besides, the classical model uses a linear relationship between mechanical and electrical domains. Then, classical bistable energy harvester equation of motion reads

$$\ddot{x} + 2\xi\dot{x} - \frac{1}{2}x(1-x^2) - \chi v = f \cos(\Omega t) \quad (1)$$

$$\dot{v} + \lambda v + \kappa \dot{x} = 0, \quad (2)$$

$$x(0) = x_0, \dot{x}(0) = \dot{x}_0, v(0) = v_0, \quad (3)$$

where x is the beam tip displacement; ξ is the damping ratio; χ is the piezoelectric coupling term in the mechanical equation (depending on the piezoceramic

properties and the structure mass); v is the voltage; λ is a reciprocal time constant ($\lambda \propto 1/R_l C_p$, where R_l is the load resistance and C_p is the equivalent capacitance of the piezoceramic layers); κ is the piezoelectric coupling term in electrical equation (depending on the piezoceramic properties and the equivalent piezoelectric capacitance); f is the external excitation amplitude; Ω is the external excitation frequency. The initial conditions are x_0 , \dot{x}_0 and v_0 , which, respectively, represent the initial values of the beam edge position, velocity, and voltage over the resistor. All these quantities are dimensionless.

The main quantity of interest (QoI) associated with the dynamical system under analysis is the mean output power given by

$$P = \frac{1}{T} \int_{t_0}^{t_0+T} \lambda v(t)^2 dt, \quad (4)$$

which is the temporal average of the instantaneous power $\lambda v(t)^2$ over a given time interval of length T .

For further, asymmetric potential, bias angle, and nonlinear electromechanical coupling are addressed in the classical harvesting model. For this purpose, introduce a quadratic nonlinearity [23, 24] to the nonlinear restoring force to characterize the asymmetric potentials. Then, the restoring force is described in linear, quadratic, and cubic terms. This essay also approached the bias angle as the external force from the self-weight of the harvester. Beyond the operation induce bias angle, [49] proposed the bias angle to repair the asymmetric potentials and enhance the harvester performance.

The nonlinear effect between material strain and the piezoelectric coefficient can be seen in piezoceramic material according to [9]. In high deformation conditions, e.g., resonance regions, it can underestimate the power harvested [17]. Therefore, models and studies considering a nonlinear electromechanical coupling for power harvesting are explored. Triplett and Quinn [48] had modeled piezoelectric coupling through a linear relationship between material deformation and piezoelectric coefficient. The authors in [46, 31] also included piezoelectric nonlinearity from higher-order terms of the elastic and electroelastic components in the constitutive piezoelectricity equation. In this way, to better calculate the energy harvested by the system, is also consider nonlinear electromechanical coupling. According to Triplett and Quinn [48] the nonlinear coupling is determined through a dependent function on the linear coupling term θ_L , nonlinear coupling term θ_{NL} , and the deformation of the piezoelectric material. It follows the dimensional piezoelectric coefficient, obtained by [48], which is represented as

$$\hat{\theta}(x) = \theta_L (1 + \theta_{NL} |x|). \quad (5)$$

The following initial value problem describes the governing lumped-parameter equation of motion for the asymmetric bistable energy harvester with bias angle and nonlinear electromechanical coupling

$$\ddot{x} + 2\xi\dot{x} - \frac{1}{2}x(1+2\delta x-x^2) - (1+\beta|x|)\chi v = f \cos(\Omega t) + p \sin \phi, \quad (6)$$

$$\dot{v} + \lambda v + (1+\beta|x|)\kappa \dot{x} = 0, \quad (7)$$

$$x(0) = x_0, \dot{x}(0) = \dot{x}_0, v(0) = v_0, \quad (8)$$

where δ is a coefficient of the quadratic nonlinearity, p is the equivalent dimensionless gravity of ferromagnetic beam, and β is the dimensionless nonlinear coupling term.

Figure 2 presents the displacement time-series for the classical bistable oscillators, with nonlinear electromechanical coupling, asymmetric potential, and bias angle. These bistable oscillators have three equilibrium points: two stable (central region of each magnet) and one unstable (between the magnets). Thus, it presents three distinct types of dynamic behavior, which mainly depend on the excitation amplitude. The lower energy orbits, i.e., oscillate only at one stable equilibrium point, are known for single-well motion. On the other side, the high-energy orbits, which oscillate between the equilibrium points (inter-well motion/ snap-through behavior), can be characterized as periodic and chaotic behaviors. In energy harvesting, vibrations in high-energy orbits can improve the system's performance. This figure also displays that piezoelectric nonlinearities, asymmetric geometry, and bias angle can change the dynamics behaviors compared to the classical one, mainly in the unstable region with a low excitation amplitude. In addition, the high sensitivity of this type of system is observed. An animation of these systems is available in the Supplementary Material and also in the STONE-HENGE code repository [14], which is shown in detail each behavior for these systems over time. The playlist at [11] also presents the linear and nonlinear harvesters' dynamic animations.

3 Global sensitivity analysis

This section presents the global sensitivity analysis background to study the bistable energy harvester dynamics. It provides relevant insights into the system in question and gives rise to model reduction schemes; for instance, it builds a simplified model by fixing relatively unimportant parameters to their nominal values and varying only the most influential parameters [38]. The global sensitivity analysis method adopted is a variance decomposition that writes the dynamical system

response as a sum of each input variable's individual and combined contributions. The Sobol indices, established in [44], are based on the variance method, quantifying the contribution of each parameter concerning the total variance of the model. It has recently been used in many works, with high impact research, as in [2,35]. One of its main advantages is dealing with nonlinear and non-parameterized models and providing a quantitative and qualitative classification.

To facilitate mathematical development, think that the QoI from the dynamical system of interest can be represented by the following functional relationship

$$Y = \mathcal{M}(\mathbf{X}), \quad \mathbf{X} = \{X_1, X_2, \dots, X_k\}, \quad (9)$$

where \mathbf{X} is an input vector with k independent parameters, that is modified by the mathematical operator \mathcal{M} , to produce the scalar output (the QoI) Y .

In this way, with aid of Hoeffding-Sobol decomposition [44,25], the QoI can be written as decomposition into summands of different dimensions

$$Y = \mathcal{M}_o + \sum_{i=1}^k \mathcal{M}_i(X_i) + \sum_{i < j} \mathcal{M}_{ij}(X_i, X_j) + \dots + \mathcal{M}_{1\dots k}(X_1 \dots X_k). \quad (10)$$

To simplify the notation, all the equations in the following assume that the input variables are uniformly defined over a support $[a_j, b_j]$, so that the support of the random input vector is $\mathcal{D}_X = \prod_{j=1}^k [a_j, b_j]$. All the sums of the expansion can be recursively computed, with the first term \mathcal{M}_o a constant equal to the expected value of Y , i.e.,

$$\mathcal{M}_o = \int_{\mathcal{D}_X} \mathcal{M}(\mathbf{X}) d\mathbf{X}. \quad (11)$$

The $\mathcal{M}_i(X_i)$ and $\mathcal{M}_{ij}(X_i, X_j)$ terms are the conditional expected value for parameter i and ij ($i \neq j$), respectively, written as

$$\mathcal{M}_i(X_i) = \int_0^1 \dots \int_0^1 \mathcal{M}(\mathbf{X}) d\mathbf{X}_{\sim i} - \mathcal{M}_o, \quad (12)$$

$$\mathcal{M}_{ij}(X_i, X_j) = \int_0^1 \dots \int_0^1 \mathcal{M}(\mathbf{X}) d\mathbf{X}_{\sim ij} - \mathcal{M}_o - \mathcal{M}_i(X_i) - \mathcal{M}_j(X_j), \quad (13)$$

where the notation \sim indicates excluded variables.

As the Eq.(10) has finitely many sums, with finite variance, it has an orthogonal decomposition property [26] in terms of conditional expectations

$$\int_{\mathcal{D}_x} \mathcal{M}_u(x_u) \mathcal{M}_v(x_v) dx = 0, \quad \forall u \neq v \quad (14)$$

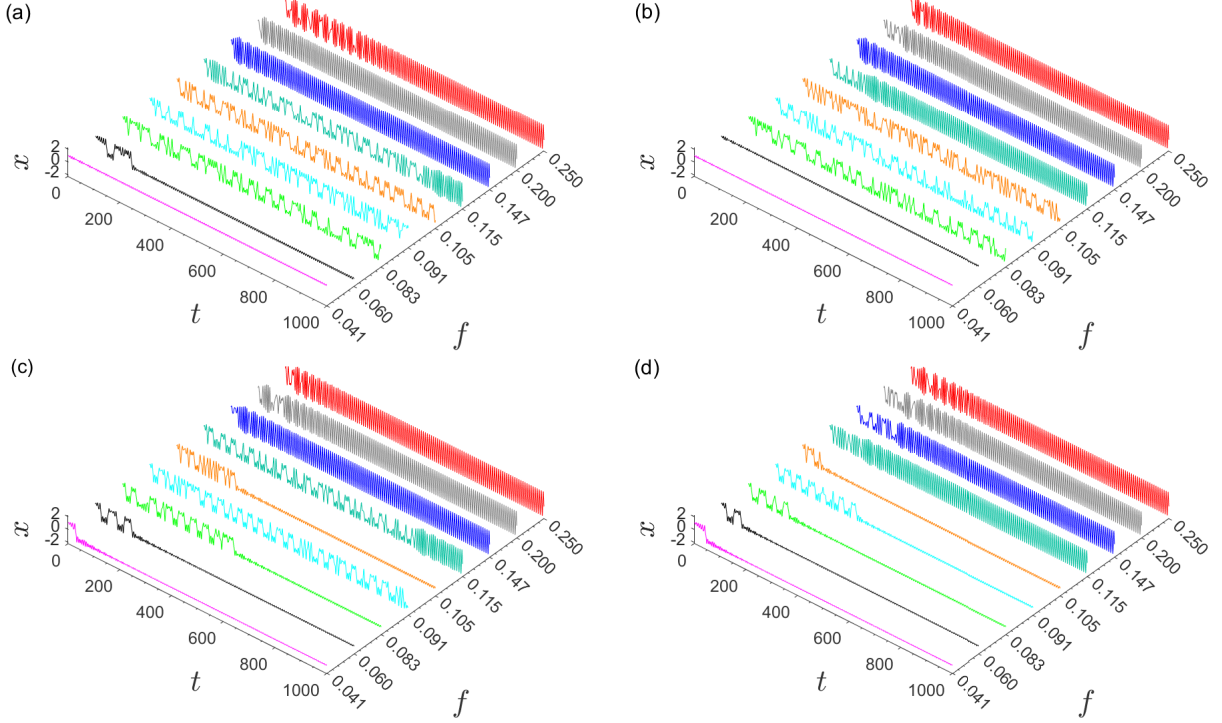


Fig. 2: The displacement time-series for different amplitude of excitation. The time-series in (a) is classical bistable energy harvester ($\beta = \delta = \phi = 0$), in (b) classical bistable energy harvester ($\beta = 1.0$ and $\delta = \phi = 0$), in (c) asymmetric bistable energy harvester ($\delta = 0.15$, $\phi = -10^\circ$ and $\beta = 0$), and in (d) asymmetric bistable energy harvester ($\delta = 0.15$, $\phi = -10^\circ$ and $\beta = 1.0$).

which $u \subset \{1, \dots, k\}$ and $x_u \stackrel{\text{def}}{=} \{x_{i_1}, \dots, x_{i_s}\}$.

Thus, it allows to meaningfully partition the system response variance and determine the Hoeffding-Sobol decomposition in terms of variance [44]. Accordingly for independent input variables, we can quantify the contribution of the individual X_i and combination $X_{ij}, \dots, X_{i\dots k}$ of variables to the total variance $Var[Y]$. By construction

$$\sum_{i=1}^k S_i + \sum_{i < j} S_{ij} + \dots + S_{12\dots k} = 1, \quad (15)$$

which indices S are called as Sobol indices.

The first-order Sobol indices

$$S_i = \frac{Var[\mathcal{M}_i(X_i)]}{Var[\mathcal{M}(\mathbf{X})]}, \quad (16)$$

quantify the additive effect of each input separately concerning the total variance, and the second-order Sobol indices S_{ij}

$$S_{ij} = \frac{Var[\mathcal{M}_{ij}(X_i, X_j)]}{Var[\mathcal{M}(\mathbf{X})]}, \quad (17)$$

compute the joint-effects of two inputs. Higher-order Sobol indices consider the interaction effects of several parameters and are written in the same way.

4 Polynomial chaos expansion

Generally, Sobol indices are calculated using the Monte Carlo (MC) simulation, but this can be computationally expensive due to the slow convergence rate of this sampling method [13, 29]. An alternative way to obtain Sobol indices is using a Polynomial Chaos Expansion (PCE) surrogate model, which is an approximate model for the original system with a short processing time, reducing the computational cost and keeping calculation accuracy [47, 10, 40].

PCE was introduced in the engineering community by Ghanem and Spanos [22] in the context of stochastic finite element analysis. The PCE is used for UQ in a wide variety of domains, e.g., in solid mechanics, thermal and fluid sciences, etc. It is a non-intrusive method representing uncertain quantities as an expansion, including the decomposition of deterministic coefficients

and orthogonal polynomial bases concerning each random variable probability distribution [52]. PCE offers an accurate and efficient way to include nonlinear effects in stochastic analysis and can be seen as an ideal mathematical way to construct and obtain a model response surface in the form of a high-dimensional polynomial in model parameters uncertain [39,43].

Assuming that the $Y = \mathcal{M}(\mathbf{X})$ is a finite variance random variable, defined in terms of the composition of the random vector \mathbf{X} and the operator \mathcal{M} , one can write the following PCE

$$Y \approx \sum_{\alpha \in \mathcal{A}} y_\alpha \psi_\alpha(\mathbf{X}), \quad (18)$$

where, ψ_α are multivariate orthonormal polynomials concerning the joint probability density function (PDF) f_X of \mathbf{X} , y_α are unknown deterministic coefficients, and the truncation set $\mathcal{A} \subset \mathbb{N}^M$ is selected from all possible multi-indices of multivariate polynomials. The unknown coefficients can be obtained from a non-intrusive least-squares regression technique, where samples from the system response are obtained from the full dynamics model.

Statistical moments and sensitivity analysis can be computed efficiently via post-processing of the surrogate model estimated coefficients. Due to orthonormality of the PCE basis, and the fact that $\psi_0 \equiv 1$ and $\mathbb{E}[\psi_\alpha(\mathbf{X})] = 0 \forall \alpha \neq 0$, the mean value and variance of the system response can be estimated as

$$\mathbb{E}[Y] \approx y_0, \quad (19)$$

and

$$\mathbb{E}[(Y - \mathbb{E}[Y])^2] \approx \sum_{\substack{\alpha \neq 0 \\ \alpha \in \mathcal{A}}} y_\alpha^2. \quad (20)$$

Similarly, the Sobol' indices of any order can also be determined analytically, e.g., the first-order indices are derived as follows

$$S_i \approx \sum_{\substack{\alpha \neq 0 \\ \alpha \in \mathcal{A}_i}} y_\alpha^2 / \sum_{\substack{\alpha \neq 0 \\ \alpha \in \mathcal{A}}} y_\alpha^2, \quad (21)$$

which truncated the PCE coefficients through parameter i for the conditional variance. The second-order Sobol' index reads

$$S_{ij} \approx \sum_{\substack{\alpha \neq 0 \\ \alpha \in \mathcal{A}_{ij}}} y_\alpha^2 / \sum_{\substack{\alpha \neq 0 \\ \alpha \in \mathcal{A}}} y_\alpha^2. \quad (22)$$

A summary of the methodology employed to address the sensibility of the system response concerning variation in the parameters is outlined in Fig. 3.

5 Results and discussion

For all numerical experiments reported here, the following nominal numerical values, i.e., free of uncertainties, are adopted for the dynamical system parameters: $\xi = 0.01$, $\chi = 0.05$, $\lambda = 0.05$, $\kappa = 0.5$, $\Omega = 0.8$ and f is varied. The initial condition is defined by $(x_0, \dot{x}_0, v_0) = (1, 0, 0)$. The dynamics is integrated by Runge Kutta scheme (4th order) over the time interval $0 \leq t \leq 2000$ with relative tolerance of 10^{-6} , and absolute tolerance of 10^{-9} . The mean output power is computed over the last 50% of these time-series.

To compute the global sensitivity analysis, it is assumed that all the system parameters are independent and uniformly distributed over given intervals, defined by a coefficient variation (*c.v.*) of $\pm 20\%$ around the nominal values.

We approached different models in order to verify specific behaviors for each condition: The classical model without nonlinear electromechanical coupling and asymmetries is evaluated. In the following, the nonlinear electromechanical coupling is included. The asymmetry bistable model with linear piezoelectric is studied. A complete model with nonlinear coupling and asymmetries is approached.

5.1 Classical bistable energy harvester

The classical bistable oscillator is sensitive to excitation conditions as well as showed in [34]. So the system's behavior through bifurcation diagrams with nominal parameters is assessed. The goal is to identify regions of the amplitude and frequency of excitation that imply distinct nominal dynamic behavior, being an essential step to sensitivity analysis. Figure 4a shows the bifurcation diagrams of the classical bistable energy harvester. The bifurcation diagram is performed sweeping the excitation amplitude to five frequency values established within the variance range. For excitation frequencies of 0.64 and 0.72, the system presents a periodic behavior for the entire amplitude range. It is possible to identify low-energy orbit regions for lower amplitude values and high-energy orbits for larger values through a phase portrait and Poincare section in Fig. 4b. Alternatively, excitation frequencies of 0.8, 0.88, and 0.96 can lead to chaotic behavior and inter-well motion.

In the sequel, two different dynamic behaviors from the bifurcation diagram are chosen to perform a sensitivity analysis using the Sobol indices, testing distinct scenarios. The first-order Sobol indices using the Monte Carlo method are calculated only twice as is an expensive process. In the following, we build and tuning the surrogate PCE model for both cases, using the Monte

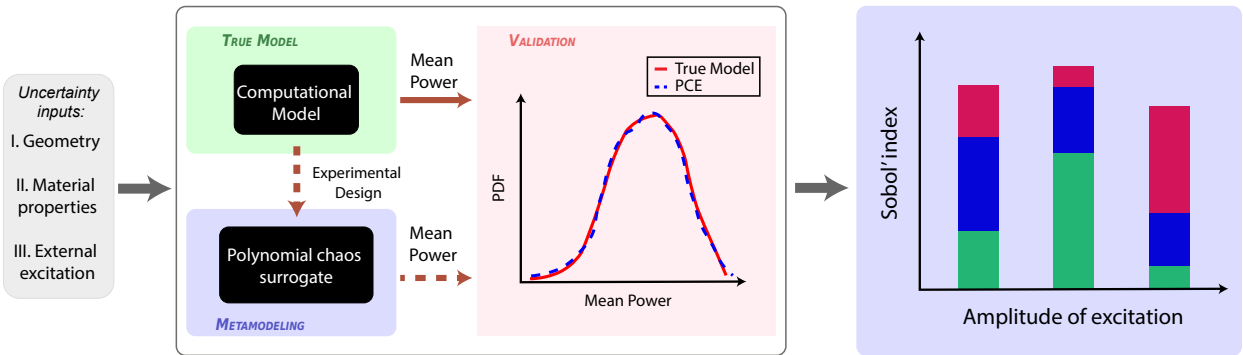


Fig. 3: Schematic representation of the methodology used to analyze the sensitivity of the energy harvester system's response to variations in its parameters.

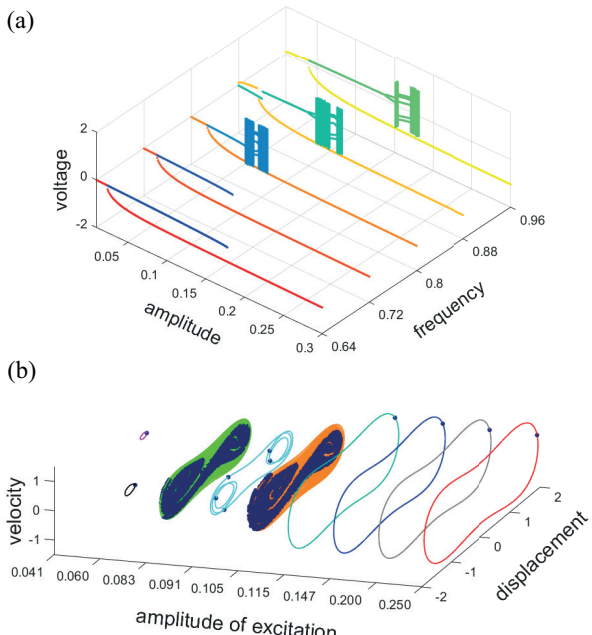


Fig. 4: Numerical simulations results for the bistable energy harvester with linear electromechanical coupling: (a) bifurcation diagrams of voltage as a function of the excitation amplitude several values of the excitation frequency. The sweeping up the amplitude excitations are presented with cool colors, while sweeping down appears in hot colors. (b) Phase portrait and Poincare section for different amplitudes of excitation and $\Omega = 0.8$.

Carlo as a reference. It is worth highlighting the PCE model requires verifying from reference to guarantee the confidentiality of convergence and accuracy, as shown in the schematic representation of the methodology, Fig. 3.

Finally, the accurately PCE model is used to explore several scenarios of excitation amplitude with low-cost processing. To illustrate this process, is selected nominal values $f = 0.147$ and $\Omega = 0.8$, as a periodic behavior and $f = 0.083$ and $\Omega = 0.8$, as a chaotic one.

The first-order Sobol indices for the periodic case are shown in Fig. 5a using MC and PCE methods. These indices reveal that 40% of the system sensitivity is due to the piezoelectric coupling acting on the electrical equation κ , then 30% for the frequency Ω , 10% for amplitude f , and 10% for the reciprocal time constant λ . The influence of the piezoelectric coupling on the mechanical system χ and the damping ratio ξ did not cause variability in power harvested.

For a second case, dealing with nominal chaotic behavior, the first-order Sobol indices are shown in Fig. 5c based on MC and PCE methods. For this scenario, the frequency and amplitude are powerful for energy-harvested variability, supplying about 40% and 20% of the total variance, respectively. The piezoelectric coupling on the electrical equation has 5%, and finally, the reciprocal time constant, piezoelectric coupling on the mechanical equation, and damping have negligible values.

To compare the employed methods, in Tab. 1 shows the Sobol Indices performance between MC and PCE for the periodic and chaotic case. Note that PCE presents a shorter time processing than MC, and the mean absolute errors (MAE) by Sobol Indices between the methods is low for both cases. Besides, the Supplementary Material presents the PCE approach by PDF compared to the complete model response, showing good performance. Then, PCE is accurate and can substitute precisely our model, becoming workable to explore several behaviors and high orders of Sobol indices.

Table 1: Comparison of the computational cost of the Sobol indices via MC and PCE methods.

case	method	sample size	CPU time* (seconds)	MAE
<i>periodic</i>	MC	10 000	$\approx 86\ 400$	1.59%
	PCE	1 000	$\approx 2\ 700$	
<i>chaotic</i>	MC	20 000	$\approx 162\ 000$	2.57%
	PCE	2 000	$\approx 6\ 000$	

*Intel i7-9750H 2.60GHz 8GB 2666GHz DDR4

Figure 5b presents the second-order indices for the first case, where they are calculated only by the validated PCE method. This result shows that only the combined excitation parameters' effect is relevant, meaning about 10% remaining of the total variance of the system. For higher orders, their evaluations are unnecessary since they have accounted for (almost) the distribution of 100% of the total variance. The second-order Sobol indices for the second case are shown in Fig. 5d and demonstrate that only the combined effect of Ω and f is relevant, about 20%. The increase of the Ω and f effects occur since chaotic behavior is more sensitive to excitation conditions, as proven in first-order Sobol indices.

A wide range of excitation amplitude using Sobol indices from the PCE model is explored. Sobol indices are calculated for each excitation amplitude, and each one is presented by the stacked bar in Fig. 5e. All the first-order indices and only relevant second-order indices are inserted. The Ω , f , and κ effects are the parameters that most cause variability in energy harvester, because present more significant indices in all range. In regions with a wide range of stability, where the system has enough energy to oscillate in inter-well motion - high excitation amplitude - the sensitivity from κ is dominant. However, Ω and f effects increase in the unstable condition, where the system can change the dynamics behaviors for a lower amplitude of excitation (as seen in Fig. 4). Furthermore, the Fig. 5e allows us to conclude that the other orders, which are the subtraction of the sum of the Sobol indices and the value one, as shown in Eq. 15, have a negligible effect.

The effects of frequency and amplitude of excitation are significant because their variability can change dynamic behaviors, which is seen in the bifurcation diagram under the $c.v. = \pm 20\%$ at high frequency. The dynamic behavior changes directly affect the power harvested, e.g., high-energy orbits produce much more electricity than chaotic or low-energy orbits. Although the frequency and amplitude of excitation are mainly responsible for behavior changes, the piezoelectric cou-

pling presents greater sensitivity for high amplitude. This is due to the small probability of behavior variation, so the piezoelectric effect predominates. Therefore, whatever scenario adjacent to the orbit changes, f and Ω are the most influential parameters; otherwise, κ is more relevant.

5.2 Classical bistable energy harvester with nonlinear electromechanical coupling

The nonlinear electromechanical coupling is added in the classical bistable energy harvester. First, a parametric investigation on nonlinear electromechanical coupling term β and amplitude excitation range through the mean power performance is performed. The result in Fig. 6 shows that the system undergoes an increase in the power harvested as β increases. However, it reaches a maximum value and damages the system performance. The high values of the nonlinear coupling term harm the power harvested for low excitation amplitude. Besides, in instability regions (chaotic behavior), the system has more significant mean power harvested changes, noticing a discontinuity color region between $f = 0.07$ to 0.105 (chaotic area). Thus, the nonlinear electromechanical coupling requires careful investigation, leading to a more complex analysis.

Figure 7 show the bifurcation diagram sweeping up and down the amplitude of excitation for different nonlinear coupling values ($\beta = 0.5, 1.0, 1.5, 2.0, 2.5$ and 3.0). The low value of nonlinear coupling maintains almost the same behavior through the absolute amplitude; to further investigation, the nonlinear coupling only decreases the chaos interval, shifting the chaos onset to higher excitation amplitudes. However, the interval chaos regions vanish as β increases, and the dynamic behavior has a large range of low-energy orbits, likewise seen in Fig. 6 with a large area of low energy as the nonlinear coupling increases (dark blue region). This effect occurs because the nonlinear coupling acts as damping in the system, as explained in [48]. Roughly speaking, the nonlinear piezoelectric configuration harvest more energy in high-energy orbits; on the other hand, it demands more external energy for the mechanical system to perform a snap-through behavior.

In Fig. 8 the leading Sobol' indices are shown for different β values with several amplitudes excitation scenarios after obtaining a PCE surrogate in the same way as done in the classical case. More detail of PCE accuracy can be seen in the Supplementary Material.

The sensitivity from the nonlinear piezoelectric term has a minor influence. However, the higher β values ($\beta \geq 2$) change the individual and combined effect of other parameters, i.e., β indirectly affects the system's

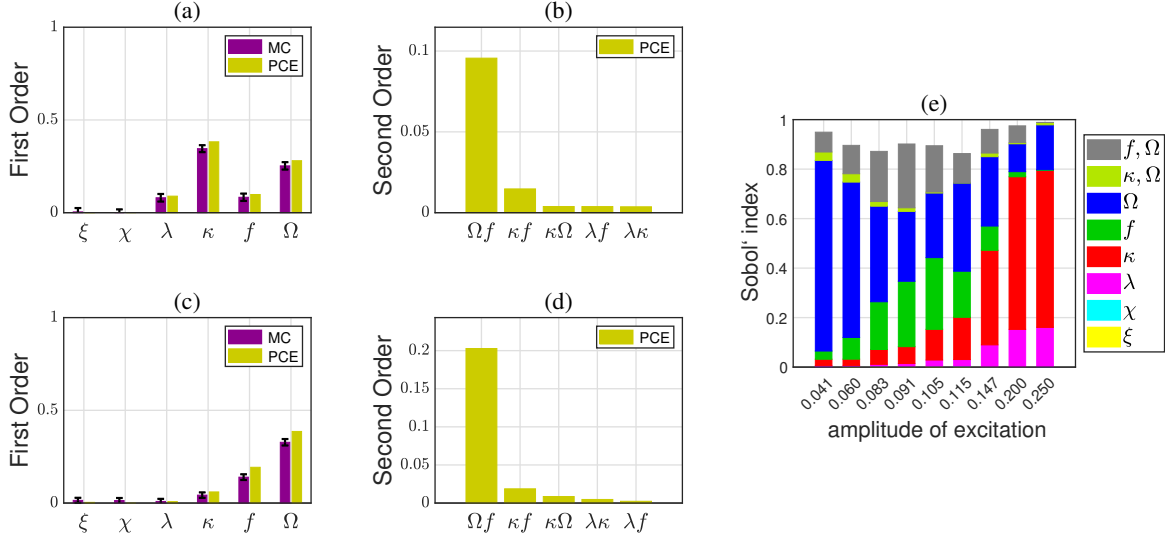


Fig. 5: Sobol' indices associated with the mean output power for the bistable energy harvester with linear coupling. First for nominal regular steady-state dynamics ($f = 0.147$ and $\Omega = 0.8$): in (a) the first-order based on MC and PCE methods and in (b) the second-order based on PCE method. Second for nominal irregular steady-state dynamics ($f = 0.083$ and $\Omega = 0.8$): in (c) the first-order based on MC and PCE methods and in (d) the second-order based on PCE method. Finally, (e) presents the main Sobol' indices exploring several scenarios with different excitation amplitudes based on the PCE method.

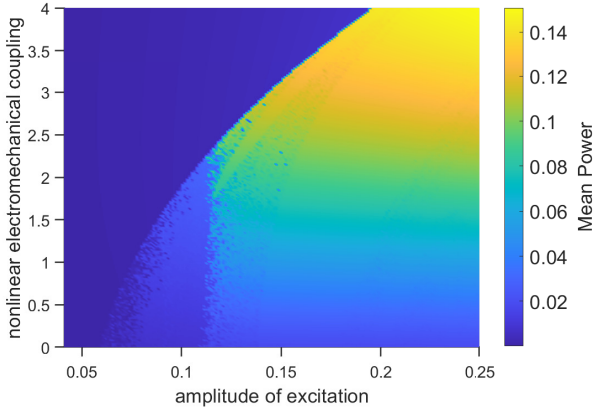


Fig. 6: Contour map of the mean output power over a wide range of excitation amplitude and nonlinear electromechanical coupling.

sensitivity. The excitation frequency's effect is dominant throughout the amplitude spectrum. The excitation amplitude has a slight influence drop since its contribution is outstanding in the chaotic regions for low values of β . The electromechanical coupling in the electrical equation has an influence reduction, mainly because the nonlinear term drives the system more sensitive to excitation conditions, as the higher β values need

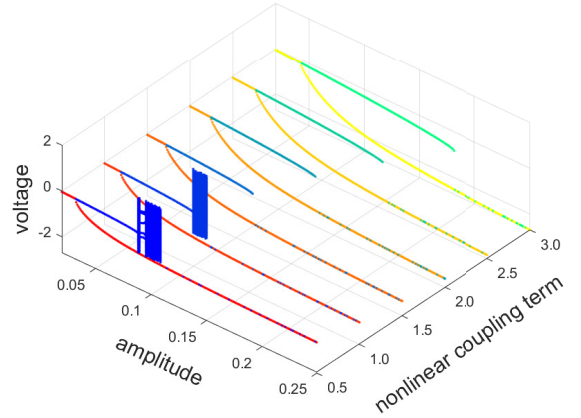


Fig. 7: Bifurcation diagrams of voltage for the bistable energy harvester with nonlinear electromechanical coupling as a function of the excitation amplitude, for six values of nonlinear coupling term: $\beta \in \{0.5, 1.0, 1.5, 2.0, 2.5, 3.0\}$ and $\Omega = 0.8$. The sweeping up the amplitude excitation is presented with cool colors while sweeping down appears in hot colors.

more external energy to perform inter-well motions and achieve a stable region. Also, there is a significant increase in the combined influence of $\Omega\beta$ and $\xi\Omega$, pre-

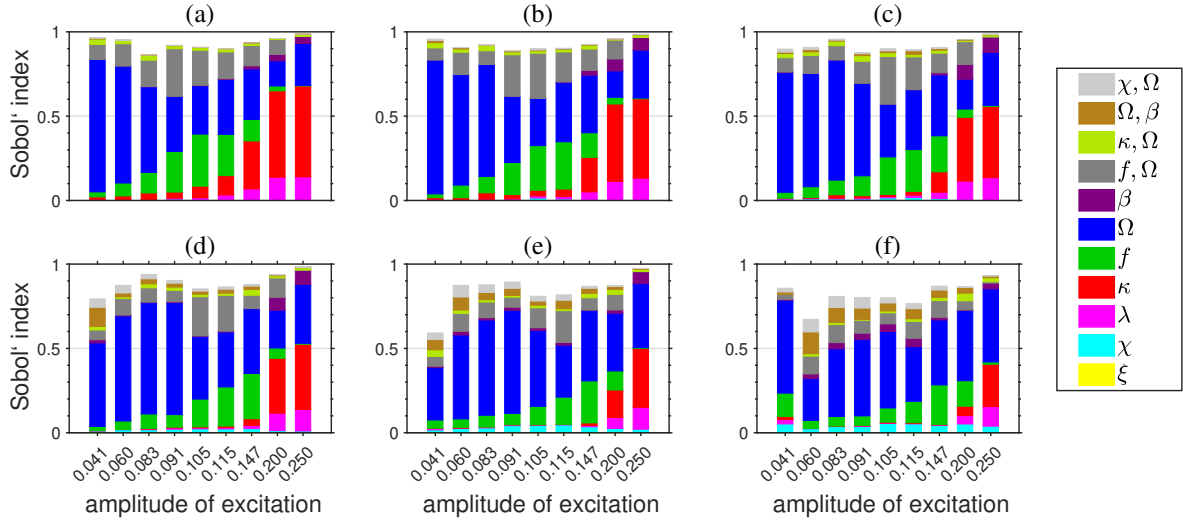


Fig. 8: Sobol indices based on PCE method associated with the mean output power of the bistable energy harvester for several scenarios of excitation amplitude with nonlinear coupling, taken into account: (a) $\beta = 0.5$, (b) $\beta = 1.0$, (c) $\beta = 1.5$, (d) $\beta = 2.0$, (e) $\beta = 2.5$, (f) $\beta = 3.0$.

viously insignificant. It concludes that when the piezoelectric nonlinearity is high, the system may change its dynamics, affecting its sensitivity and indirectly providing an increase and decrease in the individual and combined influence of other parameters. It is noteworthy that nonlinear coupling is crucial because, for low nonlinearity, it is unnecessary to worry about its uncertainties. However, for high nonlinearities, the system has a degree of indirect influence. Therefore, we recommend considering the uncertainties for high nonlinearities.

5.3 Asymmetric bistable energy harvester with linear electromechanical coupling

This section treats the classical bistable energy harvesting system considering asymmetries. The asymmetric potential, as previously discussed, is defined by a quadratic term, whereby its coefficient is unknown, as each design may have different variations. The asymmetric term is considered through a random variable described by a uniform distribution ranging from -0.15 to 0.15 . Figure 9 shows the potential energy of the system for different δ values. The δ changes the equilibrium point of the model, causing asymmetry in the potential. The left asymmetry occurs for positive values and negative values for the right asymmetry. Then, the sensitivity of the system considering the energy potential varying in this uncertainty range is analyzed.

Initially, the bias angle in the model is disregarded, i.e., $\phi = 0$. Figure 10 presents the Sobol indices for

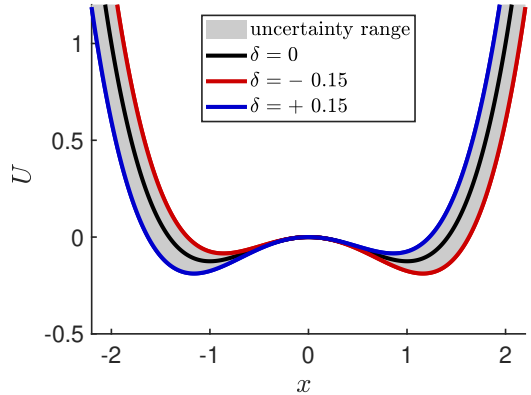


Fig. 9: Illustration of the potential energy function, of symmetric and asymmetric configurations, for δ equals to 0.15 and -0.15 . Furthermore, an uncertainty range of δ is considered.

the entire spectrum of amplitude. The quadratic nonlinearity term does not cause changes in the system's sensitivity. The excitation frequency for low amplitudes and the piezoelectric term for high amplitude influences are still dominant. Particularly significant impact coming from the δ is from second-order with the excitation frequency combined effect. However, this second-order effect is much more driven by the frequency effect than the δ itself since the frequency has a prime influence.

In the following, the bias angle is considered in the model. The bias angle ϕ is also described by a ran-

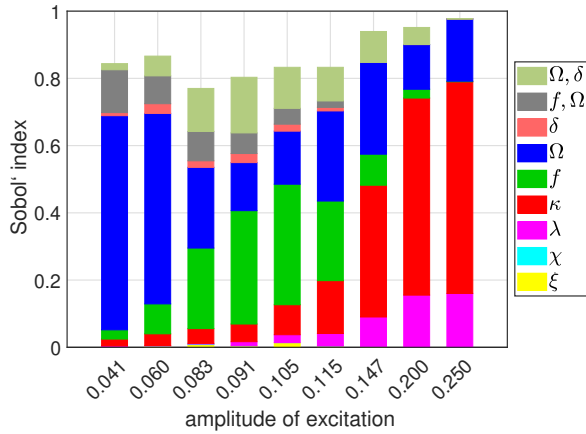


Fig. 10: Sobol indices based on PCE method associated with the mean output power of the bistable energy harvester with asymmetric potential.

dom variable with uniform distribution into -15° to 15° . Positive angles show that the system undergoes a counterclockwise rotation, and the reverse occurs for negative angles. Figure 11 shows the main Sobol indices. The bias angle presences generate a significant change in the system's sensitivity, especially in low amplitude regions, where the model exhibits dynamic instability. In this sense, at low amplitudes, the sensitivity is dominated by bias angle ϕ , excitation frequency f , and higher-order effects, chiefly of the joint parameters that already displayed high sensitivity for the first-order. The frequency effect drops on account of the bias angle higher effects, which are dominants. At high amplitude regions, the system maintains the sensitivity from the piezoelectric coupling κ . It draws attention that the asymmetry term δ keeps without relevance and can be disregarded. Therefore, beyond the care already highlighted for the excitation's parameters and electrical piezoelectric properties, the bias angle is also an important parameter that can cause variability in the model.

5.4 Asymmetric bistable energy harvester with nonlinear electromechanical coupling

Finally, the energy harvesting system considering asymmetry, bias angle, and nonlinear coupling is evaluated. It adopted the asymmetry and the bias angle terms as previously done and the nonlinear coupling equal to 1.0. Figure 12 illustrates the Sobol indices. The predominant effect from the bias angle, frequency and amplitude of excitation, and piezoelectric coupling in the electrical domain are observed. The nonlinearity coupling effects, for this scenario, do not demonstrate first

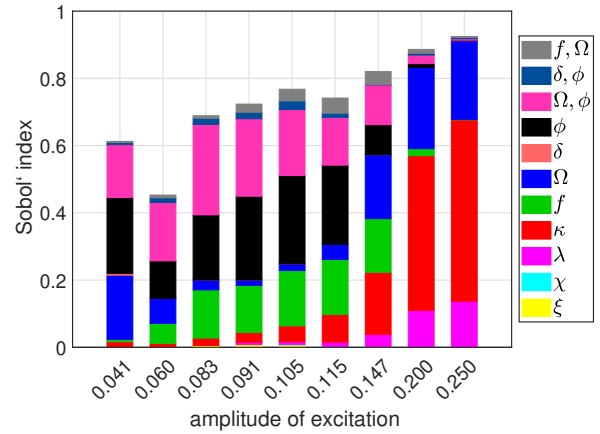


Fig. 11: Sobol indices based on PCE method associated with the mean output power of the bistable energy harvester with asymmetric potential and bias angle.

or second-order influences. Uncertainties about the asymmetry, damping, and mechanical coupling terms do not affect the power harvested, so they might be deterministic terms. As well as in the previous cases, in a low excitation amplitude region, the system is sensitive to parameters that change its behavior, driven by the excitation frequency, amplitude, and bias angle. For the high-excitation, the piezoelectric coupling linear-order effect is significant. Besides, the excitation frequency is the greatest parameter influence, smoothly overcoming the piezoelectric coupling influence. It occurs because of the nonlinear coupling term presence, which demands more external energy to achieve high orbits, as already discussed. Thus, the frequency variations become very important in changing energy orbits, confirmed by the increase in its Sobol index.

Therefore, this complete nonlinear system is still sensitive to parameters that modify the system's orbit. The analysis is complex since the piezoelectric nonlinearity presence can quantitatively change the other parameters' sensitivity. However, its uncertain effects are only significant for high amounts.

5.5 Summary of the findings

Table 2 summarizes the significant results obtained in this study. The higher-order sensitivities are controlled by high first-order influence parameters, as seen previously. Noteworthy that insensitive terms on power harvested can be deterministic variables, reducing the model order - these being the damping ξ , piezoelectric coupling in the mechanical domain χ , and asymmetric coefficient δ . In addition, it may become readily appar-

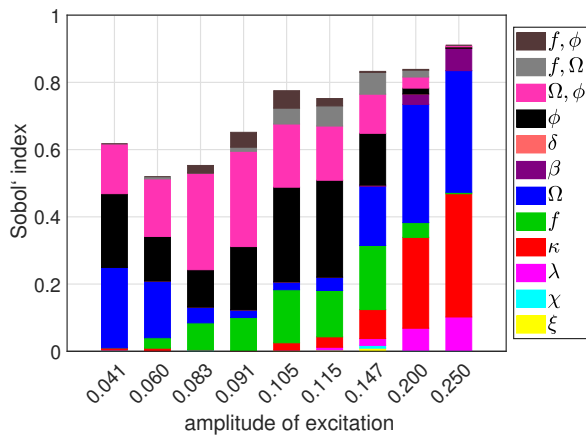


Fig. 12: Sobol indices based on PCE method associated with the mean output power of the bistable energy harvester with asymmetric potential, bias angle, and nonlinear piezoelectric coupling.

ent that the insensitivity parameters to the overall response enable manufacturing constraints to be relaxed. Parameters with medium and high sensitivity have significant influence, and given the considerations, they should be treated as stochastic variables - these being the piezoelectric coupling in the electrical domain κ , external conditions Ω and f , bias angle ϕ , nonlinear piezoelectric coupling β , and reciprocal time constant λ . Also, can associate them with optimization studies, such that minor changes in their values result in significant changes in the harvested power, becoming a proper preliminary optimization design. Then, piezoelectric coupling by electrical propriety is an innovative starting point to the enhancement process.

Figure 13 presents the uncertainty propagation of mean power in the excitation amplitude spectrum for the studied cases at different confidence levels. It is noteworthy that uncertainties were only for the sensitivities parameters, according to the table. Although remarkably, nonlinear coupling generates a higher power as already discussed, the uncertainty range is also higher than the case with nonlinear coupling, highlighting the need to verify the nonlinear term.

6 Concluding remarks

This work presented the global sensitivity analysis of a bistable energy harvesting system to identify the input parameters that lead to the most variability in the harvested power. Global sensitivity analysis based on Sobol indices, computed with the aid of a Polynomial Chaos metamodel, was employed to calculate the pa-

Table 2: Summary influence of each parameter for full bistable energy harvester

parameter	sensitivity	condition
ξ	no	-
χ	no	-
λ	low	high energy
κ	high	high energy
f	high	low and middle energy
Ω	high	all spectrum
β	low	high values
δ	no	-
ϕ	high	low and middle energy

rameters' individual and combined effect, exploring various dynamic behavior scenarios, considering that the nonlinear system allows different states-steady regimes and strange attractors. We studied a classical bistable energy harvester, then added a nonlinear electromechanical coupling and, finally, a complete model adding asymmetric term and bias angles. All these considerations are done to study a robust system and test distinct configurations models.

The results obtained here reaffirm the need to quantify and propagate uncertainties in bistable energy harvesting systems, presenting high sensitivity and a non-trivial interpretation by complex dynamic behavior. Furthermore, the framework proposes a powerful tool to develop a robust design, forecast, and optimization in bistable energy harvesting systems' performance.

Acknowledgements

The authors gratefully acknowledge, for the financial support given to this research, the following Brazilian agencies: Coordenação de Aperfeiçoamento de Pessoal de Nível Superior (CAPES) - Finance Code 001; São Paulo Research Foundation (FAPESP), grant number 19/19684-3; Brazilian National Council for Scientific and Technological Development (CNPq) grant number 306526/2019-0 ; Fundação Carlos Chagas Filho de Amparo à Pesquisa do Estado do Rio de Janeiro (FAPERJ) grants 211.304/2015, 210.021/2018, 210.167/2019, and 211.037/2019.

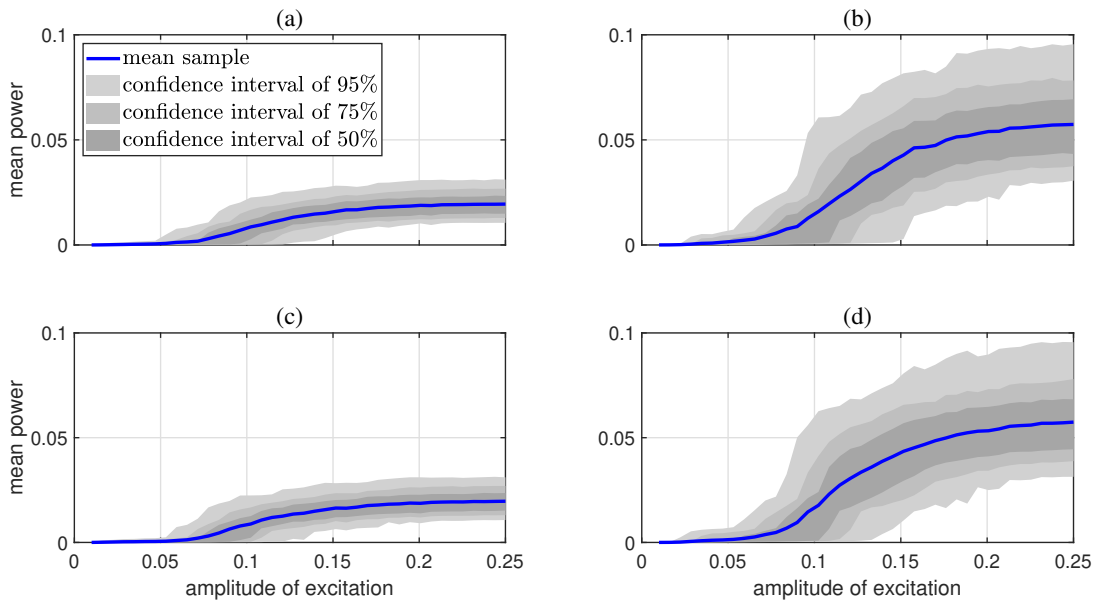


Fig. 13: Uncertainty propagation of mean power in excitation amplitude spectrum: **(a)** Classical bistable energy harvester, **(b)** Classical bistable energy harvester with nonlinear coupling ($\beta = 1$), **(c)** Asymmetric bistable energy harvester with linear coupling, **(d)** Asymmetric bistable energy harvester with nonlinear coupling ($\beta = 1$).

Code availability

The simulations reported in this paper used the computational code **STONEHENGE - Suite for Nonlinear Analysis of Energy Harvesting Systems**. To facilitate the reproduction of the results, this code is available for free in GitHub [14].

Compliance with ethical standards

Conflict of interest

The authors declare they have no conflict of interest.

References

1. Abbiati, G., Marelli, S., Tsokanas, N., Sudret, B., B. Stojadinovic, B.: A global sensitivity analysis framework for hybrid simulation. *Mechanical Systems and Signal Processing* **146**, 106997 (2021)
2. Alemazkoor, N., Rachunok, B., Chavas, D., Staid, A., Louhghalam, A., Nateghi, R., Tootkaboni, M.: Hurricane-induced power outage risk under climate change is primarily driven by the uncertainty in projections of future hurricane frequency. *Scientific Reports* **10**, 15270 (2020)
3. Aloui, R., Larbi, W., Chouchane, M.: Global sensitivity analysis of piezoelectric energy harvesters. *Composite Structures* **228**, 111317 (2019)
4. Aloui, R., Larbi, W., Chouchane, M.: Uncertainty quantification and global sensitivity analysis of piezoelectric energy harvesting using macro fiber composites. *Smart Materials and Structures* **29**, 095014 (2020)
5. Arnold, D.: Review of microscale magnetic power generation. *IEEE Transactions on Magnetics* **43**, 3940–3951 (2007)
6. Cacuci, D.: Sensitivity and uncertainty analysis: theory, vol. 1. Boca Raton: Chapman Hall/CRC, New York (2003)
7. Cao, J., Wang, W., Zhou, S., Inman, D., Lin, J.: Nonlinear time-varying potential bistable energy harvesting from human motion. *Applied Physics Letters* **107**, 143904 (2015)
8. Cottone, F., Vocca, H., Gammaioni, L.: Nonlinear energy harvesting. *Physical Review Letters* **102**, 080601 (2009)
9. Crawley, E., Anderson, E.: Detailed models of piezoceramic actuation of beams. *Journal of Intelligent Material Systems and Structures* **1**, 4–25 (1990)
10. Crestaux, T., Le Maître, O., Martinez, J.M.: Polynomial chaos expansion for sensitivity analysis. *Reliability Engineering & System Safety* **94**, 1161–1172 (2009)
11. Cunha Jr, A.: Vibration-based bistable energy harvesting system (2020). URL <https://shorturl.at/fknCO>
12. Cunha Jr, A.: Enhancing the performance of a bistable energy harvesting device via the cross-entropy method. *Nonlinear Dynamics* **103**, 137–155 (2021)
13. Cunha Jr, A., Nasser, R., Sampaio, R., Lopes, H., Breitman, K.: Uncertainty quantification through the monte carlo method in a cloud computing setting. *Computer Physics Communications* **185**, 1355–1363 (2014)
14. Cunha Jr, A., Norenberg, J., Peterson, J., Lopes, V.G.: **STONEHENGE - Suite for Nonlinear Analysis of Energy Harvesting Systems** (2021). URL <https://americocunhajr.github.io/STONEHENGE>
15. Daqaq, M., Crespo, R., Ha, S.: On the efficacy of charging a battery using a chaotic energy harvester. *Nonlinear Dynamics* **99**, 1525–1537 (2020)

16. Daqaq, M., Masana, R., Erturk, A., Quinn, D.: On the role of nonlinearities in vibratory energy harvesting: A critical review and discussion. *Applied Mechanics Reviews* **66**, 040801 (2014)
17. duToit, N., Wardle, B.: Experimental verification of models for microfabricated piezoelectric vibration energy harvesters. *AIAAJ Journal* **45** (2017)
18. Erturk, A., Hoffmann, J., Inman, D.: A piezomagnetoelectric structure for broadband vibration energy harvesting. *Applied Physics Letters* **94**, 254102 (2009)
19. Erturk, A., Inman, D.: An experimentally validated bimorph cantilever model for piezoelectric energy harvesting from base excitations. *Smart Materials and Structures* **18**, 1–18 (2009)
20. Erturk, A., Inman, D.: Broadband piezoelectric power generation on high-energy orbits of the bistable duffing oscillator with electromechanical coupling. *Journal of Sound and Vibration* **330**, 2339–2353 (2011)
21. Franco, V., Varoto, P.: Parameter uncertainties in the design and optimization of cantilever piezoelectric energy harvesters. *Mechanical Systems and Signal Processing* **93**, 593–609 (2017)
22. Ghanem, R., Spanos, P.: *Stochastic finite elements - a spectral approach*. Springer, Berlin (1991)
23. Halvorsen, E.: Fundamental issues in nonlinear wideband-vibration energy harvesting. *Physical Review E* **87**, 042129 (2013)
24. He, Q., M.F.Daqaq: Influence of potential function asymmetries on the performance of nonlinear energy harvesters under white noise. *Journal of Sound and Vibration* **333**, 3479–3489 (2014)
25. Hoeffding, W.: A class of statistics with asymptotically normal distribution. *Annals of Mathematical Statistics* **19**, 293–325 (1948)
26. Homma, T., Saltelli, A.: Importance measures in the global sensitivity analysis of nonlinear models. *Reliability Engineering & System Safety* **52**, 1–17 (1996)
27. Huang, D., Zhou, S., Litak, G.: Nonlinear analysis of multistable energy harvesters for enhanced energy harvesting. *Communications in Nonlinear Science and Numerical Simulation* **69**, 270–286 (2019)
28. Karami, M.A., Inman, D.J.: Powering pacemakers from heartbeat vibrations using linear and nonlinear energy harvesters. *Applied Physics Letters* **100**, 042901 (2012)
29. Kroese, D., Taimre, T., Botev, Z.I.: *Handbook of Monte Carlo Methods*, vol. 1. John Wiley & Sons, New Jersey (2011)
30. L., C., Orfei, Di Michele, A., Sforza, L., Franciolini, F., Gammaitoni, L.: Energy harvesting from a bio cell. *Nano Energy* **823–827**, 823 (2019)
31. Leadenham, S., Erturk, A.: Unified nonlinear electroelastic dynamics of a bimorph piezoelectric cantilever for energy harvesting, sensing, and actuation. *Nonlinear Dynamics* **79**, 1727–1743 (2015)
32. Lee, Y., Qi, Y., Zhou, G., Lua, K.: Vortex-induced vibration wind energy harvesting by piezoelectric mems device information. *Scientific Reports* **9**, 20404 (2019)
33. Li, Y., Zhou, S., Litak, G.: Uncertainty analysis of bistable vibration energy harvesters based on the improved interval extension. *Journal of Vibration Engineering & Technologies* **8**, 297–306 (2020)
34. Lopes, V., Peterson, J., Cunha Jr, A.: Nonlinear characterization of a bistable energy harvester dynamical system. In: *Topics in Nonlinear Mechanics and Physics*, vol. 228, pp. 71–88. Springer, Singapore (2019)
35. Lund, A., Dyke, J., Song, W., Bilionis, I.: Global sensitivity analysis for the design of nonlinear identification experiments. *Nonlinear Dynamics* **98**, 375–394 (2019)
36. Mann, B., Barton, D., Owens, B.: Uncertainty in performance for linear and nonlinear energy harvesting strategies. *Journal of Intelligent Material Systems and Structures* **23**, 1451–1460 (2012)
37. Mitcheson, P., Miao, P., Stark, B., Yeatman, E., Holmes, A., Green, T.: Mems electrostatic micropower generator for low frequency operation. *Sensors and Actuators A: Physical* **115**, 523–529 (2004)
38. Nagel, J., Rieckermann, J., Sudret, B.: Principal component analysis and sparse polynomial chaos expansions for global sensitivity analysis and model calibration: Application to urban drainage simulation. *Reliability Engineering & System Safety* **195**, 106737 (2020)
39. Oladyshkin, S., Nowak, W.: Data-driven uncertainty quantification using the arbitrary polynomial chaos expansion. *Reliability Engineering & System Safety* **106**, 179–190 (2012)
40. Palar, P., Zuhal, L., Shimoyama, K., Tsuchiya, T.: Global sensitivity analysis via multi-fidelity polynomial chaos expansion. *Reliability Engineering & System Safety* **170**, 175–190 (2018)
41. Ruiz, R., Meruane, V.: Uncertainties propagation and global sensitivity analysis of the frequency response function of piezoelectric energy harvesters. *Smart Materials and Structures* **26**, 065003 (2017)
42. Saltelli, A., Chan, K., Scott, E.: *Sensitivity analysis*. Wiley, New York (2000)
43. Sepahvand, K., Marburg, S., Hardtke, H.: Uncertainty quantification in stochastic systems using polynomial chaos expansion. *Inter. J. App. Mech.* **2**, 305–353 (2010)
44. Sobol, I.: Sensitivity estimates for nonlinear mathematical models. *Mathematical and Computer Modelling* **1**, 407–414 (1993)
45. Soize, C.: *Uncertainty Quantification: An Accelerated Course with Advanced Applications in Computational Engineering*, vol. 1. Springer (2017)
46. Stanton, S., Erturk, A., Mann, B., Inman, D.: Nonlinear piezoelectricity in electroelastic energy harvesters: Modeling and experimental identification. *Journal of Applied Physics* **108**, 074903 (2010)
47. Sudret, B.: Global sensitivity analysis using polynomial chaos expansions. *Reliability Engineering & System Safety* **93**, 964–979 (2008)
48. Trippett, A., Quinn, D.: The effect of nonlinear piezoelectric coupling on vibration-based energy harvesting. *Journal of Intelligent Material Systems and Structures* **20**, 1959–1967 (2009)
49. Wang, W., Cao, J., Bowen, C., Zhang, Y., Lin, J.: Nonlinear dynamics and performance enhancement of asymmetric potential bistable energy harvesters. *Nonlinear Dynamics* **94**, 1183–1194 (2018)
50. Wang, Y., Yang, E., Chen, T., Wang, J., Hu, Z., Mi, J., Pan, X., Xu, M.: A novel humidity resisting and wind direction adapting flag-type triboelectric nanogenerator for wind energy harvesting and speed sensing. *Nano Energy* **78**, 105279 (2020)
51. Xin, W., Zhang, Z., Huang, X., Hu, Y., Zhou, T., Zhu, C., Kong, X., Jiang, L., Wen, L.: High-performance silk-based hybrid membranes employed for osmotic energy conversion. *Nature Communications* **10**, 3876 (2019)
52. Xiu, D.: *Numerical Methods for Stochastic Computations: A spectral method approach*. Princeton University Press, Princeton (2010)
53. Yang, K., Fei, F., An, H.: Investigation of coupled lever-bistable nonlinear energy harvesters for enhancement of inter-well dynamic response. *Nonlinear Dynamics* **96**, 2369–2392 (2019)

54. Yi, F., Wang, X., Niu, S., Li, S., Yin, Y., Dai, K., Zhang, G., Lin, L., Wen, Z., Guo, H., Wang, J., Yeh, M., Zi, Y., Liao, Q., You, Z., Zhang, Y., Wang, Z.: A highly shape-adaptive, stretchable design based on conductive liquid for energy harvesting and self-powered biomechanical monitoring. *Science Advances* **2**, 1501624 (2016)